Tunnelling Nonlinearity of Contact of Rough Conductors in Antennas and Connectors

A. Dayan[1], Y. Huang[2], A. Schuchinsky[3]
Dept. of Electrical Engineering & Electronics, University of Liverpool, Liverpool, UK,
[1] Amir.Dayan@liverpool.ac.uk, [2] huangyi@liverpool.ac.uk, [3] aschuch@liverpool.ac.uk

***Abstract*—High-power signals are distorted by the contact nonlinearity of conductors with rough surfaces. Resistivities are obtained for a pair and array of the contact asperities in metal-insulator-metal (MIM) junctions. An improved model of the tunnelling resistivity is proposed and its accuracy is illustrated by numerical analysis. The developed model is further applied to the analysis of the thermal effect on the contact resistivity of rough conductors.**

***Index Terms*—contact resistivity, nonlinearity, passive intermodulation (PIM), signal distortion, tunnelling current**

I. Introduction

The rapidly growing amount and rate of data transmission pose major challenges to communications and navigation systems [1], [2]. The integrity of the information signals is a critical issue, which depends on the properties of materials and their contact joints at radio frequencies (RF). The linearity of the RF materials is particularly important for the design of passive devices such as antennas, filters, and multiplexers. These devices are exposed to high power at the RF front-end of smart multi-radio base stations and exhibit weakly nonlinear behaviour that results in spurious emissions [3]. Efficient mitigation of the debilitating effects of nonlinear distortions in antennas and passive components is a critical requirement for modern RF front-ends [4], [5].

Contacts and joints of good conductors with rough surfaces exhibit nonlinear behaviour when subjected to high-power RF signals [6], [7]. Antennas and passive RF devices are very sensitive to the passive nonlinearities caused by surface finish and deformations in the mechanical joints. The passive nonlinearities generate parasitic harmonics, mix frequencies, and cause passive intermodulation (PIM). They are responsible for additional noise and signal distortions in wireless and space communications systems, radars, and radio astronomy instruments [2], [8].

PIM is a nagging problem related to complex multiphysics effects. The basic mechanisms of PIM generation have been studied in contacts [9]-[12], printed transmission lines [13]-[16], cable assemblies [6], [7], [14], coaxial connectors [17], [18] and antennas [8]. The main sources of PIM in conductor joints include charge tunnelling in Metal–Insulator–Metal (MIM) junctions [9]- [12], electro-thermal effects [18], [19], and mechanical deformations of rough contact surfaces [20]-[22].

The electrical contacts of rough surfaces were studied in micro-electro-mechanical systems (MEMS) [ref?]. But the developed models are linear and limited to weak RF signals. The contact nonlinearities in conductor joints of rough surfaces were recently studied in coaxial connectors [17], [18] and waveguide flanges [22]. But weak nonlinearities and their effects on PIM in antennas and passive RF devices are tackled by mostly semi-empirical methods [23] which is not good enough.

The contact nonlinearities of rough conductors manifest themselves at several different time scales. The fastest nonlinearities are associated with the charge tunnelling and current constriction in the MIM junctions of asperities [6]. The tunnelling current strongly depends on the contact area size and thickness of an insulating layer that is determined by the contact pressure, deformation, and slightly by temperature. The mechanical deformations of the contact area and the heat flow are much slower than the charge tunnelling. Therefore, these effects on the RF signal distortions in antennas and wireless interfaces develop at significantly different time scales.

The nonlinearity of charge tunnelling through a thin insulating layer was studied first in contact junctions of good conductors. Sommerfeld and Bethe [24] examined the cases of a small and high voltage bias and an intermediate voltage bias was analysed by Holm [9]. But Holm's model was incorrect. Simmons has developed an alternative model [10], which provides a proper qualitative estimate of the resistivity of the MIM junction. But the accuracy of the Simmons model degrades when the thickness of the insulating layers is commensurate with its lattice constant. Our numerical estimates show that the error of the Simmons model can exceed 40% at the thin insulator layers or/and low heights of the potential barriers.

In this work, an advanced nonlinear model is developed for the nonlinear behaviour of the conductor joints subjected to high RF power. The model is applied to the analysis of the PIM generation by the junctions of good conductors in the base station antennas and RF front end. The model has higher accuracy and correlates well with the results of the numerical analysis. The model is further extended to account for the temperature effect on the nonlinearity of contact resistivity of conductors with rough surfaces.

II. Contact Resistance of Rough Conductors

A contact of conductors with rough surfaces is illustrated in Fig. 1. The distance Δ between the asperity bases usually varies in the range of $1-3$ μm. Asperities have random

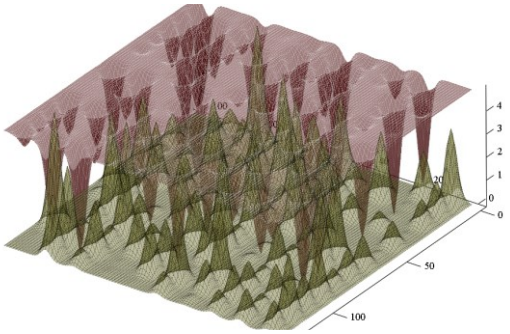

Fig. 1. Contact of two rough surfaces with random asperity heights at the surface base separation Δ.

heights and are distributed uniformly, whilst their tips are aligned vertically.

An equivalent circuit of a contact in a pair of asperities is shown in Fig. 2. It includes the asperity resistances R_{c1j}, R_{c2j}, a tunnelling resistance R_j of the insulating layer, and a contact capacitance C_j. It is important to note that $V_{Rj}(t)$ depends on the source voltage V(t) and termination load Z_L

$$V_{Rj}(t)=\frac{R_j}{R_j+R_{c12j}+Z_0}\mathrm{V}(0)\exp\left(-\Omega_j t\right)+\frac{1}{C_j\left(R_{c12j}+Z_0\right)}\int_0^t \mathrm{V}(t-\tau)\exp\left(-\Omega_j\tau\right)d\tau \quad (1)$$

where $R_{c12j}=R_{c1j}+R_{c2j}$, $\Omega_j(Z_0)=\frac{1}{C_j}\left(\frac{1}{R_j}+\frac{1}{R_{c12j}+Z_0}\right)$.

As the nonlinearity of R_j is weak, the voltage at the contact spot is determined by the linear approximation of the contact resistance R_j shown in Fig. 2. When the contact joint is subjected to the high power, the nonlinearity of R_j becomes significant, and $V_{Rj}(t)$ is calculated iteratively.

The contacts of rough surfaces with multiple asperities of random heights are represented by an equivalent circuit in Fig. 3. These contacts are modelled as the parallel connected pairs of the contact asperities. In this case, the voltage at m^{th} contact pair is calculated by taking into account the couplings between adjacent asperities

$$V_{Rjm}(t)=V_{0m}\exp\left(-Q_m t\right)+\frac{Z_0}{\zeta_N^2\eta_m}\sum_{n=1}^{N}\frac{1}{\eta_n\left(Q_m-\mu_n\right)}\left[\sum_{k=1}^{N}\frac{Z_0V_{0k}\exp\left(-\mu_n t\right)}{\eta_k R_{c12k}\left(Q_k-\mu_n\right)}+\int_0^t V(\tau)\exp\left(-\mu_n(t-\tau)\right)d\tau\right] \quad (2)$$

where V_{0m} is the voltage drop in m^{th} contact pair at t=0, $Q_m=\Omega_j(0)$, $\eta_m=C_{jm}R_{c12m}$, C_{jm}, R_{jm}, R_{c12m} are the circuit parameters of m^{th} contact pair, $\zeta_N=1+\sum_{n=1}^{N}Z_0/R_{c12n}$. μ_n are the solutions of the following algebraic system at Re $\mu_n>0$

$$\sum_{n=1}^{N}\frac{B_n}{Q_m-\mu_n}=1,\quad m=1,2,...,N \quad (3)$$

where $B_n=Z_0/\left(\zeta_N\eta_n R_{c12n}\right)$ define the asperity couplings. When surfaces are pressed together, the couplings between

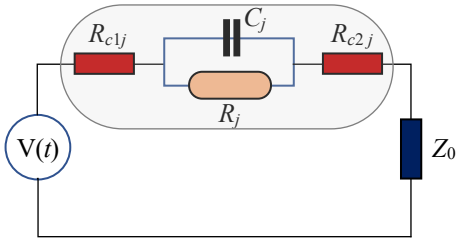

Fig. 2. Equivalent circuit of the contact of an asperity pair. R_j and C_j are the resistance and capacitance of the contact spot due to tunneling phenomenon; R_{c1j}, R_{c1j} are the conductor resistances outside contact spot due to the constriction of current; Z_0 is external load impedance; V(t) is voltage source.

nonadjacent asperity pairs are exponentially weak. Then system (3) can be reduced to the tridiagonal form, and μ_n are obtained from the solution of the successive cubic equations.

When the contacts separated by thin insulating layers are exposed to the strong RF power, their resistances R_{jm} are nonlinear due to the tunnelling effect. Then Q_m depend on $V_{Rjm}(t)$ and should be evaluated by iterations, similar to the case of a single contact pair. Owing to the inherently strong confinement of the tunnelling charges to the contact joints, the iterations converge rapidly. The tunnelling effects plays a primary role in the contact resistivity of asperities and it is discussed next.

III. TUNNELING CHARACTERSTIC

Charges tunnelling through nanoscopic oxide films at the joints of good conductors enables current flow in the MIM contacts. Probability $D(U)$ that electron with energy U pass a potential barrier $V(x)$ is usually evaluated with Wentzel, Kramers, Brillouin and Jeffreys (WKBJ) approximation [25]

$$D(U)=\exp\left(-\frac{4\pi}{h}\int_0^s\sqrt{2m\left(V(x)-U\right)H\left(V(x)-U\right)}dx\right) \quad (4)$$

where h is Planck constant, s is the width of the potential barrier, H is the Heaviside function (one for positive inputs, otherwise zero) and m is the electron mass. The potential barrier $V(x)$ can be measured from the edge of the Fermi level, so $V(x)=\eta+\varphi(x)$ where η is the Fermi level and $\varphi(x)$ is the height of the potential barrier from the Fermi level. At smooth variations of $\varphi(x)$, it can be averaged and approximated by its mean value therefore $V(x)=\eta+\bar{\varphi}$ where $\bar{\varphi}$ is the mean

barrier height above the Fermi level of the negatively biased electrode. Then $D(U)$ is reduced to [10]

$$D(U) \approx \exp\left(-A\sqrt{(\eta+\bar{\varphi}-U)H(\eta+\bar{\varphi}-U)}\right) \quad (5)$$

where $A = 4\pi s\sqrt{2m}/h$ and the current density j at a contact junction is determined by the numbers $N_1(U)$ and $N_2(U)$ of electrons tunnelling in opposite directions, transmission probability, and electron charge

$$j = e\int_0^{E_m} D(U)\left[N_1(U) - N_2(U)\right]dU \quad (6)$$

where the maximum energy E_m of electrons depends on their

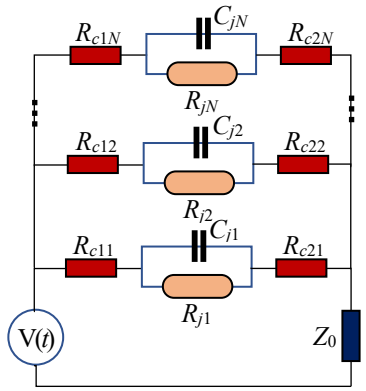

Fig. 3. Equivalent circuit of contact surfaces with N asperity pairs.

energy in an electrode because the electrons' energy levels are usually close to Fermi level, so E_m is flexible and it is chosen to be always less than potential barrier height, therefore Heaviside function can be ignored. Taking into account that $N_1(U)$ and $N_2(U)$ depend on the potential difference V_g between the contact conductors, the current density in (6) can be evaluated by using $D(U)$ approximation given in (5)

$$j(V_g) = \frac{4\pi me}{h^3}\left[\begin{array}{l} eV_g\int_0^{\eta-eV_g}\exp\left(-A\sqrt{\eta+\bar{\varphi}-U}\right)dU \\ +\int_{\eta-eV_g}^{\eta}(\eta-U)\exp\left(-A\sqrt{\eta+\bar{\varphi}-U}\right)dU \end{array}\right] \quad (7)$$

$$= \kappa\left[\begin{array}{l} \psi(\bar{\varphi}) - \psi(\bar{\varphi}+eV_g) \\ -\dfrac{A^2V_g e}{2}\left(\sqrt{\eta+\bar{\varphi}}A+1\right)\exp\left(-A\sqrt{\eta+\bar{\varphi}}\right) \end{array}\right]$$

where $\psi(\theta) = \left(\theta A^2 + 3\sqrt{\theta}A + 3\right)\exp\left(-A\sqrt{\theta}\right)$ and $\kappa = \dfrac{16\pi me}{A^4h^3}$.

In good conductors, η is much larger than $\bar{\varphi}$. Then the last term in (7) is very small and can be neglected. The remaining first 2 terms in (7) resemble Simmons model of $j(V_g)$ in [10]. But in contrast to Simmons, $\psi(\theta)$ contains additional terms $\left(3\sqrt{\theta}A+3\right)$ which play an increasingly important role in thin insulating layers of small thickness s. Namely, at $\theta = 2$ eV and insulator layers of thicknesses 0.5 nm, 1 nm, 2 nm, and 3 nm, the ratios $3\left(A\sqrt{\theta}+1\right)\Big/\left(A\sqrt{\theta}\right)^2$ are 0.41, 0.21, 0.1 and 0.07, respectively. This implies that in the case of a single crystal film of Al_2O_3 with a lattice size of 0.47591 nm 0, a relative error of Simmons model exceeds 40%.

The current densities $j(V_g)$ of MIM junction, calculated by Holm, Simmons and the refined model, are shown in Fig. 4 in comparison with the numerical analysis of the WKBJ approximation (4) with nonzero Fermi-Dirac distribution assumption and (6). It is evident that the proposed model (7) is very close to the numerical simulations and noticeably differs from the results of the Holm and Simmons models. The uncertainty of Simmons's model reduces, when the thickness of the oxide layer increases and does not exceed a few percent at low voltages and larger values of $A\sqrt{\theta}$.

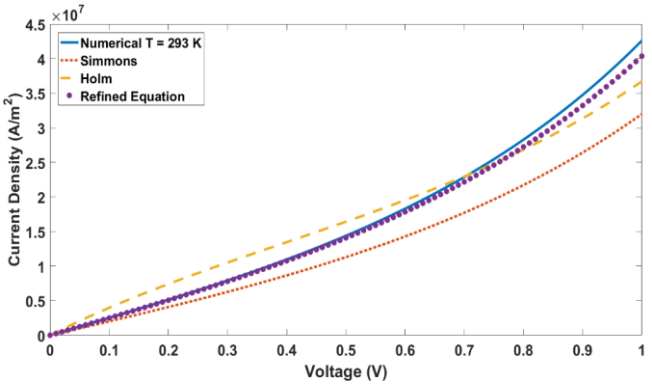

Fig. 4. Comparison of Simmons, Holm and the refined model with the numerical simulations at $\bar{\varphi} = 2$eV, s=1nm.

IV. Effect of Junction Temperature

The analytical model of contact characteristic discussed in the previous section was developed for zero temperature of the contact junction (N_1 and N_2 were temperature-independent). At higher temperatures T, the number of tunnelling charges is scaled by the normalised Fermi-Dirac distribution function

$$f(E) = \left[1+\exp\left(\frac{E-\eta}{kT}\right)\right]^{-1} \quad (8)$$

where k is Boltzmann constant and T is in Kelvins. Then the number of electrons with energy U is obtained from (8) as

$$N_1(U) = \frac{4m\pi kT}{h^3}\ln\left[1+\exp\left(-\frac{U-\eta}{kT}\right)\right]$$
$$N_2(U) = \frac{4m\pi kT}{h^3}\ln\left[1+\exp\left(-\frac{U+eV_g-\eta}{kT}\right)\right] \quad (9)$$

When $N_{1,2}(U)$ are given by (9) in case that temperature approaches zero they are converted to a Heaviside function: depending on the sign of U-η and U+eV_g-η, the current density in (6) does not have closed form and must be evaluated numerically. The simulation results in Fig. 5 show that the temperature variations of the MIM junction have a minor effect on the current density of tunnelling charges. A comparison of Fig. 4 and Fig. 5 also demonstrates that the

approximations used in the analytical models cause much larger errors than variations of ambient temperature can inflict.

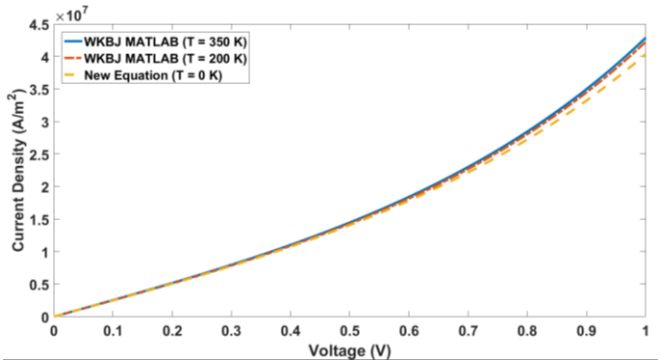

Fig. 5. Comparison of the numerical and the refined analytical solutions at different temperatures at $\bar{\varphi} = 2\,\text{eV}$, s=1nm.

V. Conclusions

Contacts of good conductors with rough surfaces have been studied in the context of their applications in antennas and passive devices of the RF front end. The improved models are devised for a single pair and an array of contact asperities. The tunnelling resistivity models of the contact joints exhibit fairly high accuracy, especially for the MIM junctions with thin insulating layers. Self-consistent analysis of the closed circuits with the source and resistive load has shown that the nonlinear contact resistivity strongly depends on the roughness of the conductor surfaces with random patterns of asperity heights. The simulation results have shown that the effect of ambient temperature on the contact resistivity of Al-Al_2O_3-Al junctions with rough surfaces is rather weak and has a minor effect on contact nonlinearity. Measurement validation is to be conducted soon and hopefully the results could be presented at the conference.

References

[1] Kanhere, O.; Rappaport, T.S. “Position Location for Futuristic Cellular Communications: 5G and Beyond”. IEEE Commun. Mag. vol. 59, 1, pp. 70–75, 2021.

[2] O. Kodheli et al. “Satellite Communications in the New Space Era: A Survey and Future Challenges”. IEEE Commun. Surv. Tutor. 1, pp. 70–109, 2021.

[3] M.Z. Waheed et al. “Passive Intermodulation in Simultaneous Transmit–Receive Systems: Modeling and Digital Cancellation Methods”. IEEE Trans. Microw. Theory Tech., vol. 68, 9, pp. 3633–3652, 2020.

[4] M. Grimm et al. “Joint Mitigation of Nonlinear RF and Baseband Distortions in Wideband Direct-Conversion Receivers”. IEEE Trans. Microw. Theory Tech., vol. 62, 1, pp. 166–182, 2014.

[5] F. Zardi, P. Nayeri, P. Rocca, Haupt, R. “Artificial Intelligence for Adaptive and Reconfigurable Antenna Arrays: A Review”. IEEE Antennas Propag. Mag., 3, pp. 28–38, 2021.

[6] Stauss, G.H. “Intrinsic Sources of IM Generation” Naval Research Lab.: Washington, DC, USA, Chapter 5, pp. 65–82, 1980.

[7] A.P. Foord, A.D. Rawlins, “A study of passive intermodulation interference in space RF hardware”. *ESTEC*, 1992**.**

[8] P. Bolli, S. Selleri, G. Pelosi, “Passive intermodulation on large reflector antennas”. IEEE Antennas Propag. Mag., 5, pp. 13–20, 2002.

[9] R. Holm, "The electric tunnel effect across thin insulator films in contacts," J. Appl. Phys., vol. 22, no. 5, pp. 569-574, 1951.

[10] J. G. Simmons, "Generalized formula for the electric tunnel effect between similar electrodes separated by a thin insulating film," J. Appl. Phys., vol. 34, no. 6, pp. 1793-1803, 1963.

[11] P. Zhang, “Scaling for quantum tunneling current in nano- and subnano-scale plasmonic junctions”. Sci. Rep, vol. 5, 09826, 2015.

[12] S. Banerjee, P. Zhang, “A generalized self-consistent model for quantum tunneling current in dissimilar metal-insulator-metal junction”. AIP Adv., vol. 9, 085302, 2019.

[13] B. A. Auld, M. Didomenico Jr., R.H. Pantell, “Traveling-wave harmonic generation along nonlinear transmission lines”. J. Appl. Phys., vol. 33, no. 12, pp. 3537–3545, 1962.

[14] M. Bayrak, F. Benson, “Intermodulation products from nonlinearities in transmission lines and connectors at microwave frequencies”. Proc. IEE, vol. 122, no. 4, pp. 361–367, 1975.

[15] A.P. Shitvov, D.E. Zelenchuk, A.G. Schuchinsky, V.F. Fusco, Passive Intermodulation Generation on Printed Lines: Near-Field Probing and Observations. IEEE Trans. Microw. Theory Tech., vol. 56, no. 12, pp. 3121–3128, 2008.

[16] J.R. Wilkerson, P.G. Lam, K.G. Gard, M.B. Steer, “Distributed passive intermodulation distortion on transmission lines”. IEEE Trans. Microw. Theory Tech., vol. 59, no. 5, pp. 1190–1205, 2011.

[17] Q. Jin et al. “Passive Intermodulation Models of Current Distortion in Electrical Contact Points”, IEEE Microw. Wirel. Comp. Lett. vol. 19, no. 3, pp. 180–182, 2019.

[18] X. Chen, L. Wang, D. Pommerenke, M. Yu, “Passive Intermodulation on Coaxial Connector Under Electro-Thermal-Mechanical Multiphysics”. IEEE Trans. Microw. Theory Tech., vol. 70, no. 1, pp. 169–177 2022.

[19] J.R. Wilkerson, K.G. Gard, A.G. Schuchinsky, M.B. Steer, “Electro-thermal theory of intermodulation distortion in lossy microwave components”. IEEE Trans. Microw. Theory Tech., vol. 56, no. 12, pp. 2717–2725, 2008.

[20] L. Kogut, K. Komvopoulos, “Analytical current-voltage relationships for electron tunneling across rough interfaces”. J. Appl. Phys. vol. 97, 073701, 2005.

[21] C. Zhai et al., “Stress-dependent electrical contact resistance at fractal rough surfaces”, J. Eng. Mech., no. 3, B4015001, 2017.

[22] C. Vicente, H.L. Hartnagel, “Passive-intermodulation analysis between rough rectangular waveguide flanges”. Microw. Theory Tech., vol. 53, no. 8, pp. 2515–2525, 2005.

[23] X. Chen, Y. He, M. Yu, D.J. Pommerenke, J. Fan, “Empirical Modeling of Contact Intermodulation Effect on Coaxial Connectors”. IEEE Trans. Instrum. Meas. vol. 69, no. 7, pp. 5091–5099, 2020.

[24] A. Sommerfeld and H. Bethe, "Handbuch der physik," Verlag Julius Springer, Berlin, vol. 1, 1933.

[25] S. Christov, "General theory of electron emission from metals," Physica Status Solidi B, vol. 17, no. 1, pp. 11-26, 1966.

"Corundum, Aluminum Oxide, Alumina, 99.9%, Al2O3." https://www.matweb.com/search/DataSheet.aspx?MatGUID=c8c56ad547ae4cfabad15977bfb537f1 (accessed 20th September, 2022).